DNA Research, 2018, 25(1), 1–10
doi: 10.1093/dnares/dsx033
Advance Access Publication Date: 7 September 2017
Full Paper

OXFORD

Full Paper

A re-sequencing-based ultra-dense genetic map reveals a gummy stem blight resistance-associated gene in *Cucumis melo*

Zhongyuan Hu[1], Guancong Deng[1], Haipeng Mou[1], Yuhui Xu[2], Li Chen[2], Jinghua Yang[1,3,4,*], and Mingfang Zhang[1,3,4]

[1]Laboratory of Germplasm Innovation and Molecular Breeding, Institute of Vegetable Science, Zhejiang University, Hangzhou 310058, China, [2]Biomarker Technologies Corporation, Beijing 101300, China, [3]Key Laboratory of Horticultural Plant Growth, Development & Quality Improvement, Ministry of Agriculture, Hangzhou 310058, China, and [4]Zhejiang Provincial Key Laboratory of Horticultural Plant Integrative Biology, Hangzhou 310058, China

*To whom correspondence should be addressed. Tel. +86 57188982123. Fax. +86 57188982123. Email: yangjinghua@zju.edu.cn

Edited by Dr. Doil Choi

Received 22 May 2017; Editorial decision 9 August 2017; Accepted 11 August 2017

Abstract

The melon (*Cucumis melo*) genome and genetic maps with hundreds to thousands of single nucleotide polymorphism markers were recently released. However, a high-resolution genetic map was lacking. Gummy stem blight (Gsb) is a destructive disease responsible for considerable economic losses during melon production. We herein describe the development of an ultra-dense genetic map consisting of 12,932 recombination bin markers covering 1,818 cM, with an average distance of 0.17 cM between adjacent tags. A comparison of the genetic maps for melon, watermelon, and cucumber revealed chromosome-level syntenic relationships and recombination events among the three *Cucurbitaceae* species. Our genetic map was useful for re-anchoring the genome scaffolds of melon. More than 92% assembly was anchored to 12 pseudo-chromosomes and 90% of them were oriented. Furthermore, 1,135 recombination hotspots revealed an unbalanced recombination rate across the melon genome. Genetic analyses of the Gsb-resistant and -susceptible lines indicated the resistance phenotype is mediated by a single dominant gene. We identified Gsb-resistance gene candidates in a 108-kb region on pseudo-chromosome 4. Our findings verify the utility of an ultra-dense genetic map for mapping a gene of interest, and for identifying new disease resistant genes.

Key words: ultra-dense genetic map, re-sequencing, gummy stem blight, *Cucumis melo*

1. Introduction

Gummy stem blight (Gsb) is a destructive disease caused by the ascomycetous fungus *Didymella bryoniae* (Auersw.) Rehm, which can infect many cucurbit species.[1] Because of the agricultural importance of this disease, cucurbit sources of genetic resistance were selected several decades ago.[2] Gsb of melon has increased in importance because it is responsible for considerable economic losses, especially in humid tropical and sub-tropical regions. Many Gsb-resistant melon varieties have been identified, and genetic analyses revealed several independent Gsb-resistance loci, including five monogenic dominant

resistance loci (*Gsb-1*, *Gsb-2*, *Gsb-3*, *Gsb-4*, and *Gsb-6*) and one monogenic recessive resistance locus (*gsb-5*) from six resistant PIs (PI140471, PI157082, PI511890, PI482398, PI420145, and PI482399), respectively.[3,4] Different molecular markers linked to Gsb resistance have been used for marker-assisted selection of Gsb-resistant germplasms.[5] However, a functional Gsb-resistance gene has not been identified.

Several genetic linkage maps from different populations have been constructed based on relatively few molecular markers, which were used to map quantitative trait loci (QTLs) for agronomic and disease-resistance traits in melon.[6–9] After the whole melon (*Cucumis melo*) genome sequence was published,[10] those available simple sequence repeat and single nucleotide polymorphism (SNP) markers were integrated to build preferably genetic maps useful for anchoring contigs/scaffolds or locating QTLs.[11] High-throughput re-sequencing has been proposed as a viable option for detecting markers, genotyping and constructing genetic maps.[12] It has been used to construct ultra-dense genetic maps based on the availability of advanced recombinant inbred lines or an F_2 population.[13–16] Many important QTLs or genes have been identified using mapping-by-sequencing methods, which have accelerated forward-genetics research even in non-model species.[17,18]

During the co-evolution of plants and microbes, host-adapted pathogens evolved effectors to suppress pathogen-associated molecular patterns-triggered immunity (PTI), which is the first basal defence against infections by non-adapted pathogens. Effector-triggered immunity (ETI) conferred by plant resistance (R) genes contributes to a highly effective defence system, which is deployed by plants as a second, largely intracellular, layer of immunity.[19–22] A coordinated relay of information between the cytoplasm and nucleus by intracellular signalling systems is required for both PTI and ETI to ensure defence-related transcripts are transferred from nucleus to the cytoplasmic protein synthesis machinery.

In this study, we constructed an ultra-dense genetic map with 12,932 recombination bin markers comprising 1,188,159 SNPs. This map may be useful for updating the melon genome and for mapping *C. melo* genes. For example, we mapped a 108-kb region associated with Gsb resistance on pseudo-chromosome 4. This ultra-dense genetic map may be useful for future molecular analyses of melon.

2. Materials and methods

2.1. Plant materials and *Didymella bryoniae* inoculation

An inbred line of *Cucumis melo* spp. *conomon* (var. *conomon*) (HS) and an inbred line of *Cucumis melo* spp. *melo* (var. *inodorus*) (XH) were crossed to generate F_1, F_2, and BC_1 populations. The HS and XH lines as well as their F_1, F_2, and BC_1 populations were used for genetic analyses. The F_2 population was used to construct a genetic map and map the candidate Gsb-resistance gene.

Plants were inoculated with *D. bryoniae* using a modified version of a published method.[23] The *D. bryoniae* spores collected from infected melon plants were cultured on potato dextrose agar medium in Petri dishes using a mycelial plug inoculation. The Petri dishes were incubated at 25 °C in the darkness for 7 days and then under ultraviolet irradiation conditions (40 w, 12 h light/12 h dark) for 4 days. Inocula were prepared by flooding the Petri dishes with 5–10 ml acidified distilled water. The resulting solution was acidified to pH 4.0 using lactic acid, and Tween-20 was added as a surfactant (20 drops/l). The spore suspension was adjusted to 5×10^5 spores/ml using a haemocytometer, and then applied to 3- to 4-week-old plants in a foliar spray. Inoculated plants were covered by a plastic tent to maintain a relative humidity of 92%. The plastic wrap was removed 3 days later. Plants were re-inoculated to ensure there were no escapees or false-positives.

2.2. Sequencing library construction and high-throughput sequencing

Genomic DNAs was extracted from the leaves of the parental lines (HS and XH) and 150 individual lines from the F_2 population according to the CTAB method. The genomic DNAs were sheared into ~500-bp fragments using the S2/E210 Ultrasonicator (Covaris, USA) for the subsequent paired-end (PE125) sequencing using the HiSeq2500 system (Illunima, USA).

2.3. SNP identification and genotyping

Raw reads were filtered to generate clean reads, which were mapped to the genome to estimate the insert sizes in the sequencing library, calculate the reads depth, and determine the distribution of reads in the melon genome (http://www.ncbi.nlm.nih.gov/assembly/GCF_000313045.1/ (23 August 2017, date last accessed))[10] using the Burrows–Wheeler Aligner programme.[24] Duplicated reads were removed using SAMtools.[25] Potential SNPs between all lines and the genome were detected using the GATK toolkit.[26] The SNPs identified between the parents were considered as polymorphic for a subsequent bin calling. The F_2 genotypes were identified based on the SNP positions. The 'pileup' function of the SAMtools programme was used to merge the SNP datasets, in which only biallelic SNPs were kept. Short reads that were matched to multiple locations in either genome, or that did not match perfectly with at least one of the parental genomes were discarded. The VCF format document was used for genotyping according to the parental SNPs, and only the aa × bb genotype was kept. The SNPs with less than 4× coverage in either parent or with fewer than 15 SNPs in a single scaffold were eliminated. Additionally, the SNPs with an extreme segregation distortion ($P < 0.01$) were initially excluded by the χ^2 test for a subsequent bin calling.

2.4. Bin map and linkage map construction

A modified slide window method was adopted for bin calling.[13] The genotype of each window was called with a window size of 15 SNPs and a step size of 1 SNP. Windows containing more than 13 'aa' or 'bb' types were genotyped as 'aa' or 'bb', respectively. Fifteen adjacent SNP intervals with the same genotype across the entire F_2 population were combined into a recombination bin. A final set of bin markers was used to construct linkage groups (LGs) with the HighMap programme.[27] Marker loci were partitioned primarily into LGs based on their locations in the *C. melo* genome. Next, the modified logarithm of odds (MLOD) scores between markers were calculated to verify the robustness of the markers in each LG. Markers with MLOD scores <5 were filtered prior to ordering. The error correction strategy of SMOOTH was then used according to the parental contributions to genotypes, and a k-nearest neighbour algorithm was applied to impute missing genotypes. Skewed markers were then added into the map by applying a multipoint maximum likelihood mapping. Map distances were estimated using the Kosambi mapping function. We then used the ALLMAPS programme to construct melon pseudo-chromosomes based on a comparison between the constructed genetic map and the map of the melon genome.[28]

Finally, we constructed pseudo-chromosomes referred to the published genome of melon.

2.5. Analysis of co-linearity and recombination hotspots

The sequences of the bin markers included in the linkage map were aligned to the physical sequences of *C. lanatus* (ftp://www.icugi.org/pub/genome/watermelon/97103/v1/ (23 August 2017, date last accessed)) and *C. sativus* (http://www.ncbi.nlm.nih.gov/genome/1639?genome_assembly_id=228904 (23 August 2017, date last accessed)) using the BLAT programme to confirm their physical positions in the genome. Spearman's rank-order correlation coefficient was calculated to assess the co-linearity between *C. melo* and *C. lanatus*, and between *C. melo* and *C. sativus*. Recombination hotspots (RHs) were predicted based on the recombination rate of markers and the anchored *C. melo* genome. If the value that the genetic distance between adjacent markers was divided by a value >20 cM/Mb, the region between the two adjacent markers was considered to be an RH.[29]

2.6. Re-anchoring scaffolds

Filtered markers were mapped to genome assembly scaffolds, and the markers on scaffolds that were mapped to pseudo-chromosomes were counted. If the value of the following equation was >0.5, we kept the scaffold mapping results, otherwise, they were eliminated: [number of markers in the largest pseudo-chromosome – number of markers in the second largest pseudo-chromosome]/number of markers in the largest pseudo-chromosome. We then determined the position of each marker relative to each other. If the relative position in the scaffold was identical to the relative position in the genetic map, the scaffold was considered to be oriented in the forward direction. Additionally, if more markers were in the forward position than in the reverse position, the scaffold was considered to be facing the forward direction. Finally, we selected one clearly oriented scaffold as the initial scaffold, and iteratively anchored other scaffolds with higher scores.

2.7. Mapping of candidate Gsb-resistance genes

The rQTL package was used to map the candidate Gsb-resistance genes. The IM method of the rQTL package was applied for qualitative trait mapping.[30] The significance thresholds were determined using 1,000 permutations, in which the threshold value was set as 2.5. The hk algorithm was selected as the me parameter, while 1 and 3 were used as the win and cofactor parameters, respectively.

2.8. RNA isolation, cDNA preparation, and quantitative real-time PCR

Leaves from HS and XH plants after inoculation (0, 0.5, 1, 2, 3, 5, and 7 days) were sampled and frozen in liquid nitrogen. Total RNA was isolated from leaves using mirVanaTM miRNA Isolation Kit (Ambion) according to the manufacturer's instructions. RNA concentration and quality were assessed using a Thermo 2000 Bioanalyzer with an RNA NanoDrop (Thermo Scientific, USA; http://www.thermo.com (23 August 2017, date last accessed)). Samples showing A260/A230 ratio of 2.0–2.2 and A260/A280 ratio of 1.8–2.0 were used for further analysis. For quantitative real-time PCR, 1 μg of total RNA was reverse transcribed to first-strand cDNA in a final reaction volume of 20 μl using miScript II RT Kit (Qiagen). The transcriptional patterns of the candidate Gsb-resistance genes were analysed using a quantitative real-time PCR (RT-qPCR). Details regarding the primers used in this study are provided in Supplementary Table S10.

2.9. Genotyping analysis of *MELO03C012987* gene

Full-length sequence of *MELO03C012987* gene (except for stop codon) was amplified by PCR from leaves of six resistant inbred lines (HP9818, HB6, HB11, HB13, CNZ, and QDH) and five susceptible inbred lines (RM, MW, DZX, M14086, and M15019) to analyse the SNP further. The primers are listed in Supplementary Table S10. The resulting PCR products were cloned into a *pEASY*-Blunt Zero Cloning Vector according to the manufacturer's instructions (TRANs, Beijing, China; www.transgen.com.cn (23 August 2017, date last accessed)) and amplified in *E coil* overnight. Subsequently, eight clones of each line were sequenced by ABI3730xl sequencer. Few clones with sequence that did not match perfectly with reference full length were discarded.

3. Results

3.1. Gsb resistance in *C. melo* is controlled by a single dominant gene

The HS and XH inbred lines were used to construct a genetic map and evaluate Gsb resistance (Fig. 1A). Plants growth and the development of disease symptoms in seedlings inoculated with *D. bryoniae* were used to assess Gsb resistance or susceptibility. Accordingly, the HS and XH inbred lines were resistant and susceptible to Gsb, respectively (Fig. 1B and Table 1). A phenotypic analysis revealed that the F_1 population from the XH × HS cross was resistant to Gsb, which is suggestive of a dominant resistance trait (Fig. 1A and Table 1). A phenotypic analysis of the F_2 population derived from the XH × HS reciprocal cross revealed a 1:3 segregation ratio for the F_2 population and a 1:1 segregation ratio for the BC_1 population, which is consistent with a monogenic resistance trait (Table 1).

3.2. Construction of a sequence-based ultra-dense *C. melo* genetic map

In total, 12.94 and 13.14 Gb clean reads were generated for the XH and HS inbred lines (26× genome coverage), respectively. Meanwhile, 217.7 Gb clean reads were generated for the 150 F_2 population individuals (2× genome coverage), with more than 85% of the bases higher than Q30 (Supplementary Table S1). The well-distributed clean reads coverage on assembly scaffolds as well as the distribution of SNP mutation and SNP quality were indicative of the stochastic nature of resequencing (Supplementary Table S1 and Figs S1 and S2). The co-segregating SNPs were clustered in recombination bins (marked as Block), which were used to construct genetic linkage map. We constructed an ultra-dense genetic map consisting of 12 pseudo-chromosomes based on 12,932 recombination bin markers comprising 1,188,159 *C. melo* SNPs (Supplementary File S1), which covered 1,818 cM, with an average distance of 0.17 cM between adjacent bin markers (Table 2, Supplementary Table S3).

Haplotype maps and linkage relationships heat maps were used to evaluate the quality of the genetic map. Haplotype maps, which indicate genotyping errors, were generated for each of the 150 lines in the F_2 population as well as the parental lines. These maps presented the recombination events (pseudo-chromosome 10 haplotype map in Supplementary Fig. S3 and all haplotype maps for the 12 pseudo-chromosomes in Supplementary File S2). Almost all the recombination blocks were completely defined, with only pseudo-chromosome 7 missing 0.01% of its data. The linkage relationships heat maps, reflected

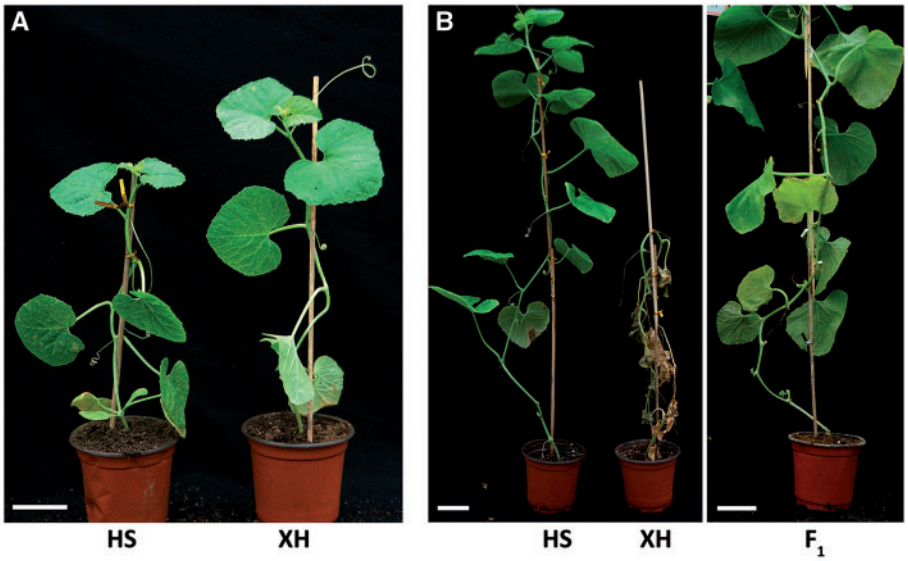

Figure 1. Phenotypic analysis of the two inbred lines used to construct a genetic map and for mapping the Gsb-resistance gene. **(A)** Phenotypes of *C. melo* spp. *conomon* (HS) and *C. melo* spp. *melo* (XH) under normal conditions. **(B)** Phenotypes of the two inbred lines and their F_1 generation after being inoculated with *Didymella bryoniae*.

Table 1. Inheritance of Gsb resistance in *C. melo*

Crosses	Generation	Resistant	Susceptible	Expected ratio (R:S)	Chi-square	*P*[a]
HS	P1	20	0			
XH	P2	0	20			
XH×HS	F_1	23	0			
XH×HS	F_2	165	54	3:1	0.013	0.91
HS×XH	F_2	81	32	3:1	0.663	0.42
(XH×HS)×XH	BC_1	47	73	1:1	5.663	0.017

Phenotypic observations for the whole plant 21 days post-inoculation were used to determine resistance/susceptible to Gsb.

[a]Observed segregation ratios are statistically consistent with the expected ratios (χ^2 test, $P < 0.05$).

Table 2. Construction of an ultra-dense *C. melo* genetic map

Pseudo-chromosome	Total maker	Total distance (cM)	Average distance (cM)	Max gap (cM)
Chr1	969	167.29	0.17	2.402
Chr2	1,041	148.75	0.14	3.74
Chr3	1,597	179.22	0.11	8.07
Chr4	1,073	226.08	0.21	12.461
Chr5	632	79.69	0.13	7.933
Chr6	1,031	164.23	0.16	4.209
Chr7	1,408	170.29	0.12	2.736
Chr8	1,469	122.15	0.08	3.138
Chr9	950	153.95	0.16	2.402
Chr10	170	79.69	0.47	20.059
Chr11	1,562	169.69	0.11	3.807
Chr12	1,030	157.15	0.15	3.071
Total/average	12,932	1818.18	0.17	20.059

the relationship between recombination markers in one pseudo-chromosome, and were used for ordering errors. These maps were created based on pair-wise recombination values for the 12,932 bin markers (pseudo-chromosome 10 linkage relationship heat map in Supplementary Fig. S4 and all linkage relationship heat maps for the 12 pseudo-chromosomes in Supplementary File S3). The constructed pseudo-chromosomes generally performed well according to the generated the heat maps.

We then compared our genetic map (HS × XH) with a published melon genetic map (PS × SC).[31] Of the 580 SNPs in the PS × SC F_2 genetic map, 558 were mapped to the HS × XH F_2 genetic map. Most of the pseudo-chromosomes were consistent with co-linearity (Fig. 2 and Supplementary Fig. S5). We likewise compared the HS × XH F_2 genetic map with the melon genetic map compiled by the International Cucurbit Genomics Initiative.[6] This comparison uncovered similar co-linear relationships among pseudo-chromosomes.

3.3. Genome re-anchoring

The HS × XH F_2 genetic map was used to re-anchor the genome scaffolds to the 12 pseudo-chromosomes. We obtained all assembled scaffolds from the melon reference genome.[10] Based on the genetic map, we anchored 92% of the scaffolds assembly (344.9 Mb of 374.8 Mb; 153 scaffolds) onto the 12 pseudo-chromosomes (Fig. 3 and Supplementary Table S4). We determined the orientation of 97.75% (336 Mb) of the anchored scaffolds, and detected chimeric scaffolds, with each anchored to different pseudo-chromosomes in the genome. For example, in scaffold NW_007546289.1, 264 Blocks were mapped onto pseudo-chromosome 5, and 72 Blocks were anchored onto pseudo-chromosome 8. In addition, in scaffold NW_007546312.1, 79 Blocks were mapped to pseudo-chromosome 8, and 41 Blocks were anchored to pseudo-chromosome 11. These results indicate that this ultra-dense genetic map may be used to improve the published melon genome assembly.

3.4. Analysis of RHs

We identified 1,135 RHs, which were unequally distributed to all 12 pseudo-chromosomes. pseudo-chromosome 9 had the most RHs (153), while pseudo-chromosome 10 had the fewest (30) (Fig. 4 and Supplementary Table S5). Most RHs were located at the telomeres of

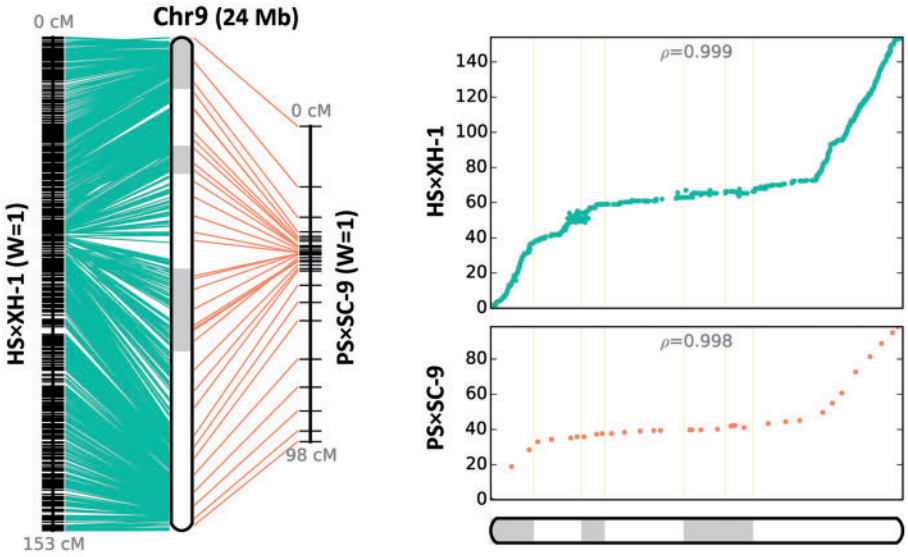

Figure 2. Constructed pseudo-chromosome (Chr9) and the co-linearity between the genetic map constructed from the HS × XH population in this study and a published genetic map for the PS × SC-9 population.

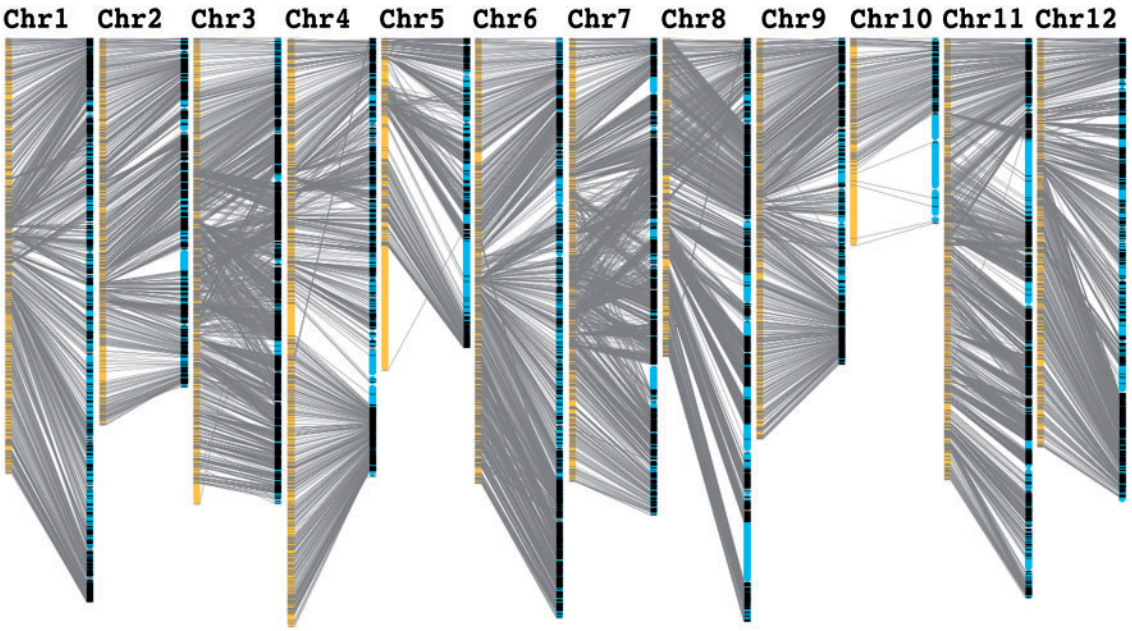

Figure 3. Re-anchored scaffolds based on the ultra-dense genetic map constructed in this study. Yellow columns represent the 12 pseudo-chromosomes of melon. Bin markers are located according to genetic distance (cM). Scaffolds were displayed in blue and grey lines represent corresponding genetic markers between each pseudo-chromosome and scaffolds.

pseudo-chromosome, which suggested the pericentromeric regions lacked recombination events (Fig. 4). The fact that almost no RHs were detected on one arm of pseudo-chromosome 10, may have been because very few markers were distributed in this region (Fig. 4), or might be related to the acrocentric morphology of this chromosome.[31]

3.5. Comparison of the *Cucurbitaceae* pseudo-chromosomes

A comparison between our genetic map of melon and the genetic maps of other *Cucurbitaceae* species (i.e., watermelon and cucumber) revealed a relatively weak syntenic relationship between the genomes (Fig. 5, Supplementary Fig. S6 and Table S6). In a comparison with cucumber chromosomes, Spearman's rank-order correlation coefficients for 12 melon pseudo-chromosomes varied from 0.63 to 0.07. Additionally, in a comparison with watermelon chromosomes, Spearman's rank-order correlation coefficients for 12 melon pseudo-chromosomes ranged from 0.67 to 0.01 (Supplementary Table S6). Of the 12 melon pseudo-chromosomes, pseudo-chromosome 10 exhibited a closer syntenic relationship with watermelon Chr 5 and cucumber Chr 5 than the other pseudo-chromosomes (Fig. 5 and Supplementary Table S6). These results imply that the genomic

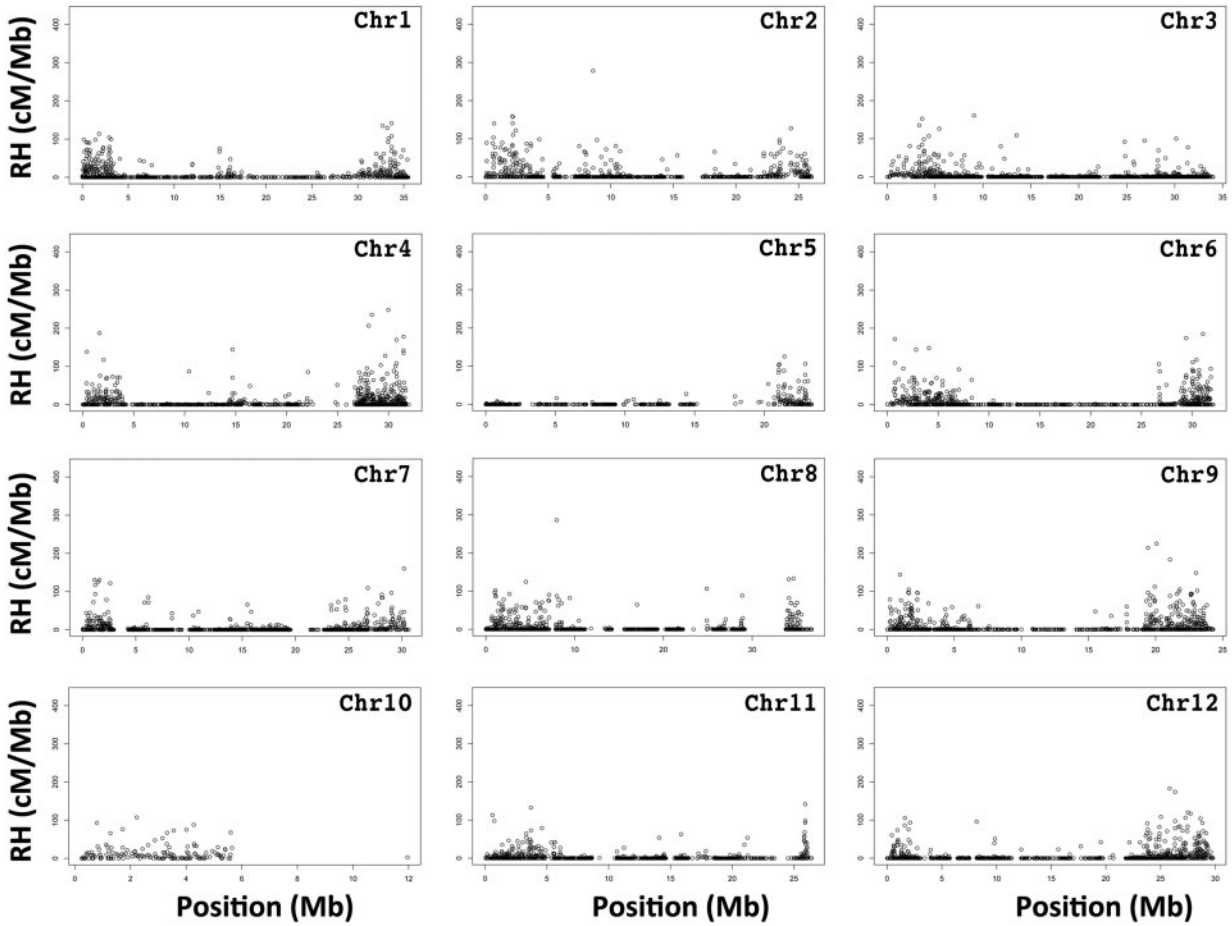

Figure 4. Genetic positions of the recombination hotspots in the 12 melon pseudo-chromosome.

structures of pseudo-chromosome 10 from melon, Chr 5 from watermelon and cucumber are relatively conserved.

3.6. Mapping of *C. melo* Gsb-resistance gene candidates

The 12 pseudo-chromosomes as well as the genotyping and phenotyping data related to Gsb resistance were used to map the candidate Gsb-resistance gene (*GsbR*). We identified a 0.667-cM region on pseudo-chromosome 4 with two bin markers (Block13188 and Block13179) that satisfied the LOD threshold of 2.5, implying the region is linked to Gsb resistance. The LOD values of Block13188 and Block13179 were 2.528 and 2.737, respectively, while the contribution rates were 9.36 and 10.72, respectively (Fig. 6A and Supplementary Table S7). The additive effects and dominant effects were 0.177 and 0.12, respectively (Supplementary Table S7). Furthermore, a scaffold (CM3.5_scaffold00018) with 71 well-distributed SNPs was identified during the genotyping of the HS (Gsb resistant) and XH (Gsb susceptible) parent lines (Supplementary Table S8). Eight candidate genes were annotated in this region based on the melon reference genome, GO, NR, Swiss-Prot, COG, and KEGG databases (Fig. 6A, Table 3, and Supplementary Table S9).

We analysed the expression patterns of these candidate genes in HS and XH plants inoculated with *D. bryoniae*. We were unable to detect the expression of *MELO3C012988*, *MELO3C012989*, and *MELO3C012990* in control and inoculated plants, implying these genes may not directly influence Gsb-resistance. In contrast, *MELO03C012987* expression was considerably upregulated in HS and XH plants inoculated with *D. bryoniae* (Fig. 6B). The expression levels of the remaining candidate genes (i.e., *MELO3C012986*, *MELO3C012991*, *MELO3C012992*, and *MELO3C012993*) were not induced by *D. bryoniae* inoculation (Fig. 6B). These results indicated that *MELO03C012987* is most likely the gene responsible for Gsb-resistance in melon. A Pfam BLAST analysis indicated that MELO03C012987 includes a DUF761 domain (Fig. 6C). We then compared the mapped region between the HS and XH lines. A non-synonymous SNP was identified in the *MELO03C012987* gene, which resulted in a Lysine being replaced by a glutamic acid in the encoded protein (Fig. 6D). Genotyping *MELO03C012987* from six resistant and five susceptible inbred lines of *C. melo* revealed that all five susceptible lines (RM, MW, DZX, M14086, and M15019) exhibited Adenine at the non-synonymous SNP, which is same as that found in XH plant. Of the six resistant lines genotyped, five (HB6, HB11, HB13, CNZ, and QDH) had the Guanine at this non-synonymous substitution as that in HS plant. Whereas, HP9818 exhibited either Guanine or Adenine, representing a heterozygous genotype (Fig. 6E and Supplementary Table S11).

4. Discussion

The melon genome sequence[10] and several genetic maps[7,8,11,31] have recently been published. However, functional genomics studies

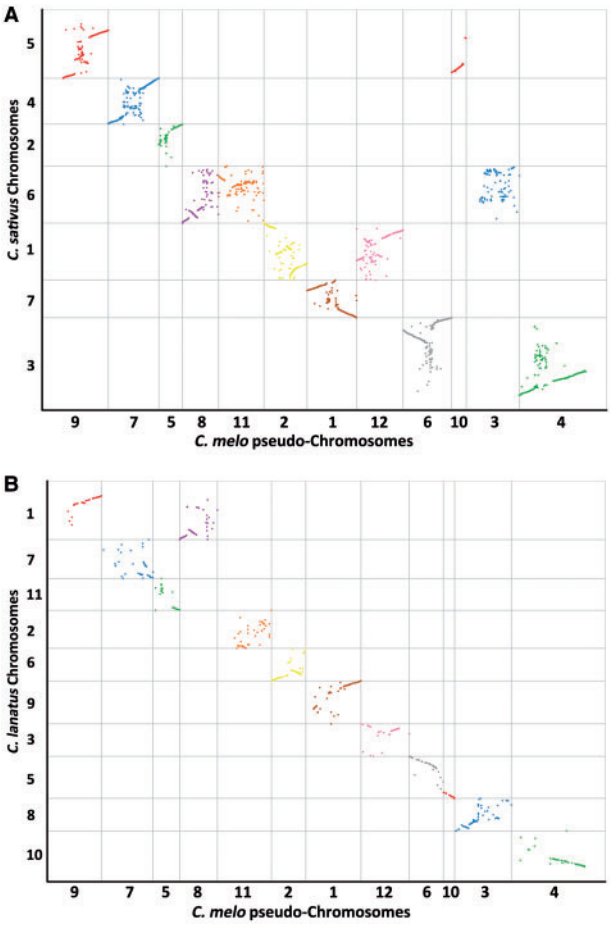

Figure 5. Comparison of the syntenic relationships among the pseudo-chromosomes of *C. melo,* and chromosomes of *C. sativus* and *C. lanatus*. (**A**) Syntenic relationships between *C. melo* and *C. sativus*. (**B**) Syntenic relationships between *C. melo* and *C. lanatus*.

involving melon are still restricted by the fact only a few hundred or thousand markers have been explored. Based on a F_2 population of double-haploid DHL92 used for melon genome sequence,[10] a genetic map was developed composing of 580 SNPs, which anchored the scaffolds into a chromosome-scale pseudomolecules.[31] This work not only provided a significantly updated melon genome, but also indicated that high-resolution genetic map could be an efficient approach for the improvement of genome draft sequence. Rapid advances in high-throughput sequencing have revolutionized SNP marker discovery and genotyping analyses. Additionally, high-throughput sequencing-based approaches are now routinely used to construct genetic maps.[13,15,16] An important strength of genotyping-by-sequencing (GBS) is that the detection and genotyping of genome-wide SNP markers occur simultaneously. Moreover, a GBS approach does not require a reference genome for SNP calling and genotyping. However, an available reference genome is useful because it enables the proper alignment and ordering of sequenced tags and helps to impute low-coverage data.[32] These two sub-species are commonly used in breeding programmes because they are resistant to multiple diseases and exhibit desirable traits regarding sugar content and flavour. After a genotyping analysis, we obtained 12,932 bin markers, which included more than one million SNPs. Using these bin markers, we constructed the first ultra-dense genetic map that can be used as a reference in future studies of melon. Recently, 354.98 Mb of melon scaffolds were anchored and 325.4 Mb of sequences were oriented by a new set of targeted SNP markers with better distribution in the parents of the DHL92 melon reference genome.[31] In our study, several missed scaffolds were assembled into melon pseudo-chromosome. Furthermore, more sequence (336.05 Mb) were oriented in our new scaffold genome, suggesting that our ultra-dense genetic map could further improve the anchoring and orienting of melon scaffold genome assembly.

A GBS-based high-resolution genetic map can be efficiently used to identify genetic regions and candidate genes underlying agronomically important traits.[17,33,34] We mapped a 0.667 cM region on pseudo-chromosome 4, and identified eight candidate genes for Gsb resistance in this region. Thus, an ultra-dense genetic map can be constructed and candidate genes underlying Gsb resistance can be mapped using a GBS approach. Genetic map-based high-quality reference genome sequences provide useful information not only for identifying genes and regulatory elements, but also for characterizing genomic diversity.[35] Our ultra-dense genetic map improved the re-anchoring of scaffolds to the reference genome. It may also contribute fundamental information for the *de novo* assembly of a high-quality oriental melon genome. Moreover, the improved anchoring of scaffolds may help researchers analyse chromosomal structures to improve the accuracy of gene mapping. Comparisons of genetic maps can reveal the genetic basis for conserved and variable sequences within species or among related species. We observed a strong co-linearity, but also rearrangements between our HS × XH F_2 genetic map and the genetic maps of whole-genome sequenced melons, especially in pseudo-chromosomes 3–5. A chromosome-level comparison between the *C. melo* genetic map and the *C. sativus* and *C. lanatus* genomes revealed syntenic relationships among these three *Cucurbitaceae* species. The complex syntenic patterns presented as segmented chromosome-to-chromosome orthologous relationships were consistent with the notion that the chromosomal evolution and rearrangement among these three *Cucurbitaceae* species is very complex.[10,36,37] However, it remains possible that such differences are derived from different mapping populations being used for various genotypes associated with a chromosome-level reorganization.

Among the detected Gsb-resistance candidate genes, *MELO3C012986* encodes a protein similar to a VHS domain-containing protein, which is involved in clathrin-related endomembrane trafficking in plants.[38] *MELO3C012991* encodes a Sec13, which is part of a nuclear pore complex with subunits that are involved in the responses to pathogens, cold stress, auxin, and ethylene.[39] We identified an *RT*-like gene (i.e., encoding a reverse transcriptase) upstream of *Sec13*. An RT gene is usually associated with a mobile element, such as a retrotransposon, retrovirus, group II intron, retron, or retroplasmid, as well as an occasional retro (pseudo) gene.[40–42] *MELO3C012992* encodes a GATA zinc finger transcription factor family gene (GATA TF4-like), which has been implicated in light-responsive, circadian-regulated, and nitrate-dependent control of transcription.[43,44]

Plants are often attacked by pathogens and have evolved a multi-layered defence system. An essential defence mechanism involves the expression of resistance (*R*) genes, which enables plants to detect pathogens carrying the corresponding avirulence (*Avr*) genes.[21] The R protein-mediated pathogen recognition can be direct or indirect via the action of effectors (Avr proteins) on host targets. The *R* gene-based resistance is usually considered to be related to gene-for-gene resistance, which often involves a hypersensitive response (HR). *MELO3C012987* encodes a protein that is similar to the uncharacterized Avr9/Cf-9 rapidly elicited (ACRE) protein 146, which is related

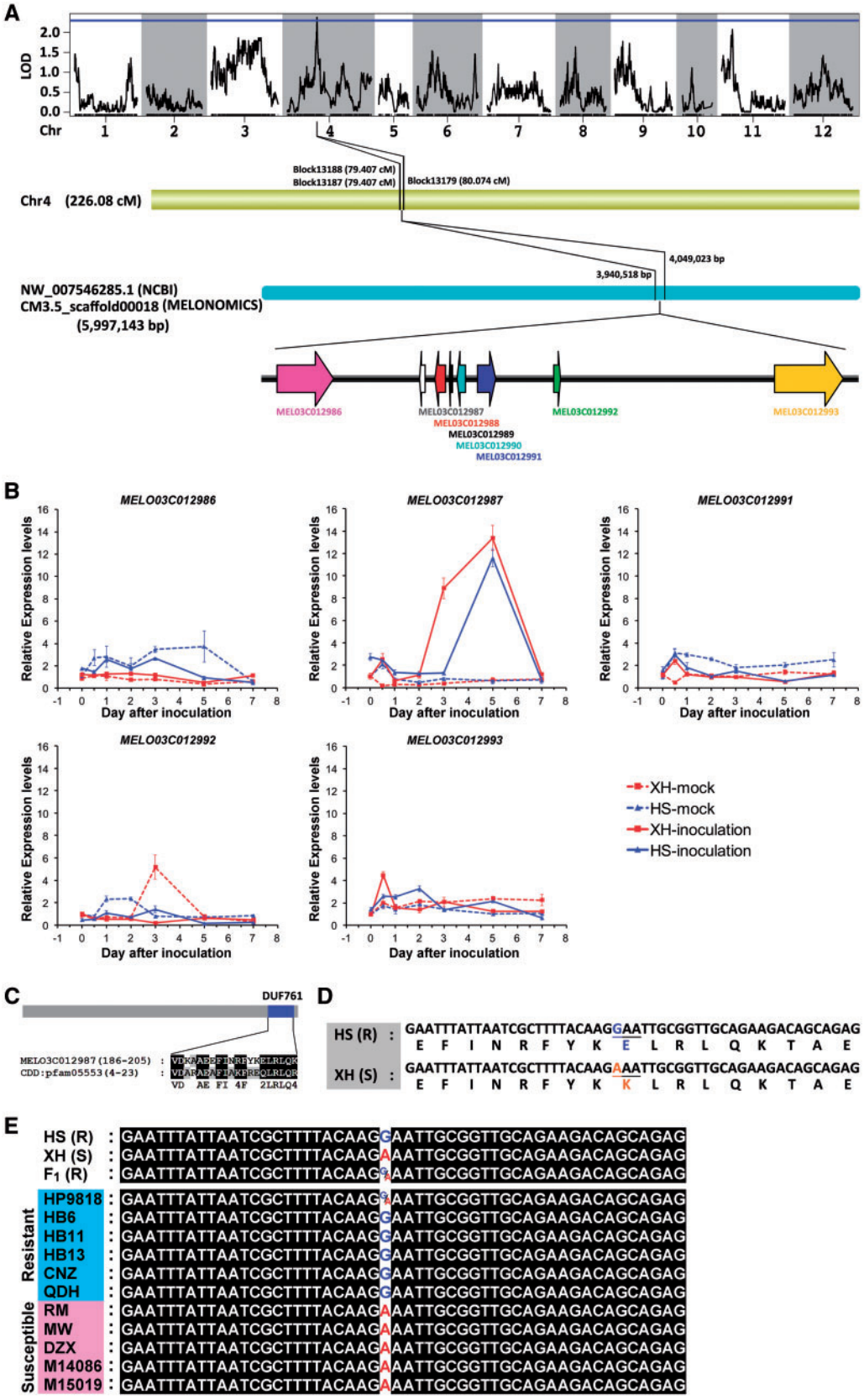

Figure 6. Mapping of *C. melo* Gsb-resistance candidate genes. (**A**) Mapping of Gsb-resistance candidate genes. (**B**) Analysis of Gsb-resistance candidate gene expression levels in plants inoculated with *Didymella bryoniae*. (**C**) DUF761 domain in *MEL03C012987* gene. (**D**) A non-synonymous SNP in the *MELO03C012987* gene. (**E**) Genotyping of the non-synonymous substitution of *MEL03C012987* in resistant and susceptible lines of *C. melo*.

Table 3. Annotation of Gsb-resistance candidate genes

Gene ID	Location	Direction	Annotation	Expression
MELO3C012986	3934220–3943507	+	Similar to VHS domain-containing protein	Expressed
MELO3C012987	3957629–3958543	−	Similar to uncharacterized *Avr9/Cf-9* rapidly elicited protein 146	Expressed
MELO3C012988	3960154–3961860	−	Similar to putative ribonuclease H protein	ND
MELO3C012989	3962492–3963050	−	*LINE-1* retrotransposable element ORF2 protein	ND
MELO3C012990	3963801–3965186	−	uncharacterized protein	ND
MELO3C012991	3967157–3970154	+	Similar to Protein *SEC13* homolog	Expressed
MELO3C012992	3979703–3980781	+	Similar to GATA transcription factor 9	Expressed
MELO3C012993	4015998–4027273	+	Similar to Biotin–protein ligase	Expressed

to the gene-for-gene dominant resistance to fungal pathogens.[45,46] Many ACRE genes encode putative signalling components, suggesting they are essential for early defence responses.[45] Four genes (i.e., *ACRE74*, *ACRE189*, *ACRE264*, and *ACRE276*) have been confirmed as essential for both Cf-9- and Cf-4-mediated HR. Previous studies determined that *ACRE74*, *ACRE264*, and *ACRE276* are critical for the Cf-9-mediated resistance to C. *fulvum*.[47–49] Our data suggested that *MELO3C012987*, which encodes a protein similar to ACRE146, might be the Gsb-resistance gene in melon.

In conclusion, our ultra-dense genetic map may be useful for future studies aimed at identifying the genes regulating agronomically important melon traits. Additionally, functionally characterizing *MELO3C012987* may contribute to the development of new strategies to control Gsb in *Cucurbitaceae* species. However, gene-based disease resistance sometimes fails because of developmental and/or environmental changes. Incorporating Gsb resistance into field-grown crops will require the development of sustainable broad-spectrum disease resistance.

Availability

The re-sequence data can be available at NCBI under accessions SRP114921.

Acknowledgements

We would like to thank Prof Fengming Song from Institute of Biotechnology, Zhejiang University, to offer the Gsb isolate.

Supplementary data

Supplementary data are available at *DNARES* online.

Funding

This study was supported by grants from the earmarked fund for Modern Agro-Industry Technology Research System of China (CARS-26-17), the Science and Technology Program of Zhejiang Province (2017C32041), and the Breeding Alliance of Rice and Major Economic Crops of Zhejiang University.

Conflict of interest

None declared.

References

1. Keinath, A.P. 2011, From native plants in Central Europe to cultivated crops worldwide: the emergence of Didymella bryoniae as a Cucurbit Pathogen. *Hortscience*, **46**, 532–5.
2. Sitterly, W.R. 1972, Breeding for disease resistance in Cucurbits. *Annu. Rev. Phytopathol.*, **10**, 471–90.
3. Frantz, J.D. and Jahn, M.M. 2004, Five independent loci each control monogenic resistance to gummy stem blight in melon (*Cucumis melo* L.). *Theor. Appl. Genet.*, **108**, 1033–8.
4. Wolukau, J.N., Zhou, X.H. and Chen, J.F. 2009, Identification of amplified fragment length polymorphism markers linked to gummy stem blight (Didymella bryoniae) resistance in Melon (*Cucumis melo* L.) PI 420145. *Hortscience*, **44**, 32–4.
5. Bi, Y., Xu, B., Qi, C., et al. 2015, Pryamiding disease resistance genes and variety improvment by molecular marker-assisted selection in melon (*Cucumis melon* L.). *Sci. Agric. Sin.*, **48**, 523–33.
6. Diaz, A., Fergany, M., Formisano, G., et al. 2011, A consensus linkage map for molecular markers and quantitative trait loci associated with economically important traits in melon (*Cucumis melo* L.). *BMC Plant Biol.*, **11**, 111.
7. Harel-Beja, R., Tzuri, G., Portnoy, V., et al. 2010, A genetic map of melon highly enriched with fruit quality QTLs and EST markers, including sugar and carotenoid metabolism genes. *Theor. Appl. Genet.*, **121**, 511–33.
8. Yuste-Lisbona, F.J., Capel, C., Sarria, E., et al. 2011, Genetic linkage map of melon (*Cucumis melo* L.) and localization of a major QTL for powdery mildew resistance. *Mol. Breeding*, **27**, 181–92.
9. Chang, C.W., Wang, Y.H. and Tung, C.W. 2017, Genome-wide single nucleotide polymorphism discovery and the construction of a high-density genetic map for melon (*Cucumis melo* L.) using genotyping-by-sequencing. *Front. Plant Sci.*, **8**, 125.
10. Garcia-Mas, J., Benjak, A., Sanseverino, W., et al. 2012, The genome of melon (*Cucumis melo* L.). *Proc. Natl. Acad. Sci. U.S.A.*, **109**, 11872–7.
11. Diaz, A., Forment, J., Argyris, J.M., et al. 2015, Anchoring the consensus ICuGI genetic map to the melon (*Cucumis melo* L.) genome. *Mol. Breeding*, **35**, 188.
12. Davey, J.W., Hohenlohe, P.A., Etter, P.D., Boone, J.Q., Catchen, J.M. and Blaxter, M.L. 2011, Genome-wide genetic marker discovery and genotyping using next-generation sequencing. *Nat. Rev. Genet.*, **12**, 499–510.
13. Huang, X.H., Feng, Q., Qian, Q., et al. 2009, High-throughput genotyping by whole-genome resequencing. *Genome Res.*, **19**, 1068–76.
14. Xua, X.Y., Zeng, L., Tao, Y., et al. 2013, Pinpointing genes underlying the quantitative trait loci for root-knot nematode resistance in palaeopolyploid soybean by whole genome resequencing. *Proc. Natl. Acad. Sci. U.S.A.*, **110**, 13469–74.
15. Wang, S., Chen, J., Zhang, W., et al. 2015, Sequence-based ultra-dense genetic and physical maps reveal structural variations of allopolyploid cotton genomes. *Genome Biol.*, **16**, 108.
16. Mun, J.H., Chung, H., Chung, W.H., et al. 2015, Construction of a reference genetic map of *Raphanus sativus* based on genotyping by whole-genome resequencing. *Theor. Appl. Genet.*, **128**, 259–72.
17. Candela, H., Casanova-Saez, R. and Micol, J.L. 2015, Getting started in mapping-by-sequencing. *J. Integr. Plant Biol.*, **57**, 606–12.
18. Schneeberger, K. 2014, Using next-generation sequencing to isolate mutant genes from forward genetic screens. *Nat. Rev. Genet.*, **15**, 662–76.
19. Chisholm, S.T., Coaker, G., Day, B. and Staskawicz, B.J. 2006, Host-microbe interactions: shaping the evolution of the plant immune response. *Cell*, **124**, 803–14.

20. Dodds, P.N. and Rathjen, J.P. 2010, Plant immunity: towards an integrated view of plant-pathogen interactions. *Nat. Rev. Genet*., **11**, 539–48.
21. Jones, J.D.G. and Dangl, J.L. 2006, The plant immune system. *Nature*, **444**, 323–9.
22. Tsuda, K. and Katagiri, F. 2010, Comparing signaling mechanisms engaged in pattern-triggered and effector-triggered immunity. *Curr. Opin. Plant Biol*., **13**, 459–65.
23. Kwon, M.K., Hong, J.R., Sun, H.J., Sung, K.Y., Cho, B.H. and Kim, K.C. 1997, Standardization of a mass production technique for pycnidiospores of *Didymella bryoniae*, gummy stem blight fungus of Cucurbits. *Korean J. Plant Pathol*., **13**, 105–12.
24. Li, H. and Durbin, R. 2009, Fast and accurate short read alignment with Burrows-Wheeler transform. *Bioinformatics*, **25**, 1754–60.
25. Li, H., Handsaker, B., Wysoker, A., et al. 2009, The sequence alignment/map format and SAMtools. *Bioinformatics*, **25**, 2078–9.
26. DePristo, M. A., Banks, E., Poplin, R., et al. 2011, A framework for variation discovery and genotyping using next-generation DNA sequencing data. *Nat. Genet*., **43**, 491–8.
27. Liu, D.Y., Ma, C.X., Hong, W.G., et al. 2014, Construction and analysis of high-density linkage map using high-throughput sequencing data. *PLoS One*, **9**, e98855.
28. Tang, H.B., Zhang, X.T., Miao, C.Y., et al. 2015, ALLMAPS: robust scaffold ordering based on multiple maps. *Genome Biol*., **16**, 3.
29. Zhang, J., Zhang, Q.X., Cheng, T.R., et al. 2015, High-density genetic map construction and identification of a locus controlling weeping trait in an ornamental woody plant (*Prunus mume* Sieb. et Zucc). *DNA Res*., **22**, 183–91.
30. Broman, K.W. and Sen, S. 2009, *A guide to QTL mapping with Q/qtl*. Springer, New York.
31. Argyris, J.M., Ruiz-Herrera, A., Madriz-Masis, P., et al. 2015, Use of targeted SNP selection for an improved anchoring of the melon (*Cucumis melo* L.) scaffold genome assembly. *BMC Genomics*, **16**, 4.
32. Poland, J.A. and Rife, T.W. 2012, Genotyping-by-sequencing for plant breeding and genetics. *Plant Genome-Us*, **5**, 92–102.
33. Verma, S., Gupta, S., Bandhiwal, N., Kumar, T., Bharadwaj, C. and Bhatia, S. 2015, High-density linkage map construction and mapping of seed trait QTLs in chickpea (*Cicer arietinum* L.) using genotyping-by-sequencing (GBS). *Sci. Rep.-Uk*, **5**, 17512.
34. Lee, J., Izzah, N.K., Choi, B.S., et al. 2016, Genotyping-by-sequencing map permits identification of clubroot resistance QTLs and revision of the reference genome assembly in cabbage (*Brassica oleracea* L.). *DNA Res*., **23**, 29–41.
35. Feuillet, C., Leach, J.E., Rogers, J., Schnable, P.S. and Eversole, K. 2011, Crop genome sequencing: lessons and rationales. *Trends Plant Sci*., **16**, 77–88.
36. Guo, S.G., Zhang, J.G., Sun, H.H., et al. 2013, The draft genome of watermelon (*Citrullus lanatus*) and resequencing of 20 diverse accessions. *Nat Genet*., **45**, 51–82.
37. Huang, S.W., Li, R.Q., Zhang, Z.H., et al. 2009, The genome of the cucumber, *Cucumis sativus* L. *Nat. Genet*., **41**, 1275–U1229.
38. Zouhar, J. and Sauer, M. 2014, Helping hands for budding prospects: ENTH/ANTH/VHS accessory proteins in endocytosis, vacuolar transport, and secretion. *Plant Cell*, **26**, 4232–44.
39. Parry, G. 2013, Assessing the function of the plant nuclear pore complex and the search for specificity. *J. Exp. Bot*., **64**, 833–45.
40. Schulman, A.H. 2013, Retrotransposon replication in plants. *Curr. Opin. Virol*., **3**, 604–14.
41. Gladyshev, E.A. and Arkhipova, I.R. 2011, A widespread class of reverse transcriptase-related cellular genes. *Proc. Natl. Acad. Sci. U.S.A*., **108**, 20311–6.
42. Toro, N. and Nisa-Martinez, R. 2014, Comprehensive phylogenetic analysis of bacterial reverse transcriptases. *Plos One*, **9**, e114083.
43. Reyes, J.C., Muro-Pastor, M.I. and Florencio, F.J. 2004, The GATA family of transcription factors in Arabidopsis and rice. *Plant Physiol*., **134**, 1718–32.
44. Manfield, I.W., Devlin, P.F., Jen, C.H., Westhead, D.R. and Gilmartin, P.M. 2007, Conservation, convergence, and divergence of light-responsive, circadian-regulated, and tissue-specific expression patterns during evolution of the Arabidopsis GATA gene family. *Plant Physiol*., **143**, 941–58.
45. Stergiopoulos, I. and de Wit, P.J.G.M. 2009, Fungal effector proteins. *Annu. Rev. Phytopathol*., **47**, 233–63.
46. Grennan, A.K. 2006, Plant response to bacterial pathogens. Overlap between innate and gene-for-gene defense response. *Plant Physiol*., **142**, 809–11.
47. Rowland, O., Ludwig, A.A., Merrick, C.J., et al. 2005, Functional analysis of Avr9/Cf-9 rapidly elicited genes identifies a protein kinase, ACIK1, that is essential for full Cf-9-dependent disease resistance in tomato. *Plant Cell*, **17**, 295–310.
48. Nekrasov, V., Ludwig, A. A. and Jones, J. D. G. 2006, CITRX thioredoxin is a putative adaptor protein connecting Cf-9 and the ACIK1 protein kinase during the Cf-9/Avr9-induced defence response. *FEBS Lett*., **580**, 4236–41.
49. van den Burg, H.A., Tsitsigiannis, D.I., Rowland, O., et al. 2008, The F-box protein ACRE189/ACIF1 regulates cell death and defense responses activated during pathogen recognition in tobacco and tomato. *Plant Cell*, **20**, 697–719.